# NASA TECHNICAL NOTE

NASA TN D-3647

# TEST OF A LARGE-DIAMETER
# RING-STIFFENED CYLINDER SUBJECTED
# TO HYDROSTATIC PRESSURE

*by Donaldson A. Dow and James P. Peterson*

*Langley Research Center*
*Langley Station, Hampton, Va.*
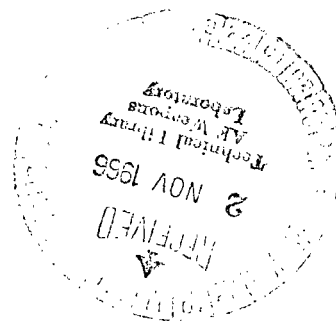
# TEST OF A LARGE-DIAMETER RING-STIFFENED CYLINDER

## SUBJECTED TO HYDROSTATIC PRESSURE

By Donaldson A. Dow and James P. Peterson

Langley Research Center
Langley Station, Hampton, Va.

# TEST OF A LARGE-DIAMETER RING-STIFFENED CYLINDER
## SUBJECTED TO HYDROSTATIC PRESSURE

By Donaldson A. Dow and James P. Peterson
Langley Research Center

## SUMMARY

Results of a buckling test of a 10-foot-diameter (3-meter) ring-stiffened cylinder loaded "hydrostatically" with air pressure are presented. The cylinder failed as a result of wall buckling at a pressure of approximately 76 percent of the pressure computed with the use of classical small-deflection buckling theory. Since both the computed and experimental buckling pressures were considerably less than that predicted with the use of contemporary design equations, a serious shortcoming of the design equations is revealed.

## INTRODUCTION

Very few experimental data are available on stiffened cylindrical shells that fail from hydrostatic external pressure at the low values of pressure of interest in aerospace structures. Those data that are available (refs. 1 and 2, for example) were obtained on cylinders with widely spaced stiffeners so that local buckling of the skin preceded general failure of the cylinder. More desirable structures have closely spaced stiffeners so that general failure is expected to occur before, or perhaps at, the load for which skin buckling is expected.

The purpose of the present investigation is to present test results for a hydrostatically loaded, 10-foot-diameter (3-meter), ring-reinforced cylinder and to compare the results with those predicted with the use of design equations for such structures. In addition, shortcomings in contemporary design analyses are discussed.

## SYMBOLS

The units used for physical quantities defined in this paper are given both in U.S. Customary Units and in the International System of Units (SI) (ref. 3). Factors relating the two systems for the units used in the present investigation are presented in the appendix.

$A_O$            area of end ring

$A_R$      area of reinforcing ring

$D_x$      bending stiffness of orthotropic cylinder wall in axial direction

$E$      Young's modulus

$E_x, E_y$      extensional stiffness of orthotropic cylinder wall in axial and circumferential direction, respectively

$l$      ring spacing

$m$      number of half waves in cylinder buckle pattern in axial direction of cylinder

$n$      number of full waves in cylinder buckle pattern in circumferential direction of cylinder

$p$      pressure

$p_{ult}$      applied pressure at failure of cylinder

$\cdot R$      radius of cylinder

$t$      skin thickness of cylinder

$w$      radial displacement of cylinder wall caused by deformation under load or by initial imperfections

$x$      axial coordinate

$\epsilon_x$      strain in axial direction

$\mu$      Poisson's ratio of wall material

$\mu_x, \mu_y$      Poisson's ratio associated with bending of orthotropic wall of cylinder in axial and circumferential direction, respectively

$\mu_x'$      Poisson's ratio associated with extension of orthotropic wall of cylinder in axial direction

## TEST SPECIMEN AND TEST PROCEDURE

General features of the test cylinder are depicted in figure 1 and details of construction are given in figure 2. The numerical values presented in figure 2 for the wall-thickness and reinforcing-ring dimensions represent an average of a large number of measurements; nominal values are given for the remaining dimensions. The cylinder was constructed from 2024-T3 aluminum-alloy sheet material. It had eight longitudinal wall splices consisting of lap joints held together by double lines of seam welds and had four circumferential splices in each of its 36 reinforcing rings (fig. 2). The circumferential location of splices in individual rings was adjusted so that splices did not occur at the same location for all rings. The rings were spotwelded to the wall of the cylinder with 3/32-inch-diameter (2.4-mm) spots spaced at approximately 1/4 inch (6.3 mm).

The hat-section rings were preformed from flat sheet material in a power brake and then roll formed into rings. In the establishment of the roll-forming procedure, an attempt was made to produce rings which were free of any visible waviness. The attempt was not entirely successful, however, as can be seen from figure 1(c), which indicates that the tops of the hats appear wavy (buckled) in some sections of the cylinder.

The test cylinder had geometric deviations (initial imperfections) from the desired cylindrical form before application of load. The deviations were determined with the use of a scanner, especially built for such purposes, which autographically plotted deviation as a function of axial location on the cylinder as the scanner was moved along a generator of the cylinder. Input to the two axes of the plotter was achieved with the use of a linear variable differential transformer-type displacement transducer and with a 10-turn potentiometer. Typical plots, which represent approximately 1/4 of the cylinder circumference, are presented in figure 3. The plots were obtained at successive 6-inch (15.2-cm) intervals around the circumference of the cylinder. Deformations are measured from an imaginary surface formed by the approximate circles corresponding to the weld lines (between cylinder wall and reinforcing ring) nearest each end of the cylinder and the straight-line generators connecting the two circles.

The surface of the test cylinder appears rather irregular in the plots of figure 3; irregularities that have a depth of a skin thickness or more are prevalent. Note that two of the more severe irregularities were instrumented with strain gages in order to study behavior of the cylinder in the vicinity of the imperfections as the cylinder was subjected to load.

The cylinder was loaded by slowly evacuating the air from inside the cylinder with the use of a mechanical vacuum pump. Resistance-type wire strain gages were mounted on the cylinder at various locations prior to testing, and strains from the gages were recorded during the test with the use of the Langley central digital data recording facility.

Data from the gages were used to study the strain distribution in the cylinder and to help determine the cause of buckling of the cylinder.

Typical material properties were used in reducing data from the tests. Young's modulus E was taken to be 10 600 ksi (73.1 GN/m$^2$) and Poisson's ratio $\mu$ was assumed to be 0.32.

## TEST RESULTS

Selected strain-gage data from gages mounted on the test cylinder are given in figure 4. The data represent an average of the strain measured by "back-to-back" gages in some instances and denote the data from individual gages in others. The location of three of the gage stations is indicated in figure 3; the remaining two stations fall outside the bounds of the plots of figure 3. Note that the locations include two stations near rather severe imperfections (buckles), one which is buckled outward (location A) and one which is buckled inward (location B). Strain data from these two locations suggest that the imperfections increased in depth as load was applied to the cylinder. Imperfection growth was particularly pronounced at the higher pressures. Strain data from the gages at more normal locations of the cylinder are more in line with calculated strains, although measured circumferential strains are generally somewhat greater than calculated strains. This behavior suggests that the test cylinder wall was not as stiff in the circumferential direction as calculations would indicate, presumably because imperfections lower wall stiffness. On the other hand, measured axial strains agree reasonably well with calculated strains.

Although not shown in figure 4, individual strain-gage readings indicated considerable wall bending at several locations. The bending indicated by the data for gage locations A and B supports the conclusion that the imperfections at these locations grew with applied load, as noted earlier. For some of the other locations, bending was also indicated by individual strain-gage readings from gage pairs 1 and 2 as well as from gage pairs 3 and 4 and indicated that the wall at those locations experienced growth of local deformations.

Failure of the test cylinder appears to be the result of general buckling over the complete cylinder; all the strain data indicate considerable nonlinearity at loads approaching ultimate load.

Approximate calculations of the prebuckling deformations of the test cylinder were made in order to understand more fully the behavior of the cylinder under load. Results of the calculations are shown in figure 5. Figure 5(a) shows the deformation of a typical wall section somewhat removed from the ends of the cylinder. The calculations were made with the aid of the equations of reference 4 and the assumption of equally spaced rings of half the area and at half the spacing of the actual rings. A sketch of the idealized

4

structure is given in figure 5(a). Note that the skins of the actual cylinder and the idealized cylinder are supported at the same number of locations. The calculations (which also were used to locate the calculated curves in fig. 4) indicate that the central portion of the cylinder was relatively free from axisymmetric prebuckling deformations arising from reinforcing rings.

Calculated prebuckling deformations near the ends of the cylinder are shown in figure 5(b) for both a simply supported and a clamped condition at the end ring. The calculations were made with equations similar to those of reference 4 but rederived for a cylinder with orthotropic wall properties. The following approximations for orthotropic wall properties were used in the calculations:

$$E_x = Et$$

$$E_y = E\left(\frac{A_R}{l} + t\right)$$

$$D_x = \frac{Et^3}{12}$$

$$\mu'_x = \mu\frac{E_x}{E_y}$$

and the additional approximation that the product $\mu_x\mu_y$ is small compared with unity. Figure 5(b) indicates that axisymmetric deformations near the end ring reach a magnitude of approximately one skin thickness and decay rapidly with distance from the end of the cylinder. The calculations also indicate that the area of the end ring was sufficiently large to suppress radial deformations at that station.

The failed cylinder is shown in figure 6. Failure occurred suddenly and was accompanied by a loud resounding noise. During failure considerable crimping and tearing occurred and small pieces of the cylinder were thrown free of the cylinder. Although not apparent from figure 6, the appearance of the failed cylinder suggested that buckling in a mode with $m = 1$ and $n = 5$ or $6$ may have caused failure. Calculations that were made do not support this suggestion; the calculations indicate that failure was initiated in a mode in which $m$ was large ($\approx 39$) and $n$ was equal to zero (axisymmetric mode).

Figure 7 illustrates the results of calculations made to determine the buckling mode of the test cylinder; the calculations were made with the use of the stability equation of reference 5. Note the two minimums, one at $m = 1$ and the other at $m = 39$. The minimum at $m = 39$ represents the calculated buckling mode of the cylinder. Failure probably initiated in a mode similar to the calculated mode but augmented by initial imperfections or other undefined discrepancies between the ideal calculated cylinder and the actual cylinder, and then passed into the observed mode as deformation in the calculated mode

reduced the various wall stiffnesses of the cylinder. Transition from the calculated mode to the observed mode possibly occurred rapidly and could not be observed. The calculated buckling pressure is almost the same as that which would be obtained for the m=39,n=0 mode if pressure on the curved walls of the cylinder were neglected and the cylinder were considered to be subjected only to axial compression. The cylinder failed at a differential pressure of 5.71 psi (39.4 kN/m$^2$) which is 76 percent of the calculated pressure.

The reason for the 24-percent discrepancy between theory and test has not been established in this investigation but is probably a result of several phenomena. Initial imperfections and prebuckling deformations probably contribute to the discrepancy. Both deformations have been shown to have amplitudes of a skin thickness or more and both are known to be important factors in the buckling of isotropic cylinders under axial load. (See investigations of refs. 6 to 8, for example.) Buckling of the test cylinder was evidently caused primarily by axial load, and investigations similar to those for isotropic cylinders would be expected to yield comparable results for ring-reinforced cylinders. Another contributing factor to the 24-percent discrepancy may be associated with the small difference between the ring spacing (36 rings) and the calculated axial wavelength of buckles (39 half waves); in the buckling theory, the contribution of the rings is assumed to be "smeared out" over the ring spacing (ref. 5). This assumption is probably unconservative but again the quantitative effect of the assumption is not known. Lastly, figure 1(c) indicates that the tops of some of the hat-section rings were prebuckled by fabrication stresses. The buckled hats are less stiff than similar unbuckled hats and may contribute to the discrepancy between theory and test.

Two stabilizing effects not taken into account in the buckling calculation should be mentioned: (1) the effect of the hat-section rings in contributing to the bending stiffness $D_x$ and hence to increasing the calculated buckling pressure and (2) the effect of the resistance of the reinforcing rings to the rolling action imposed by axisymmetric buckling deformations. These effects are neglected in the analysis of reference 5 because they are normally small, particularly for cylinders with open-section stiffeners that buckle into an asymmetric mode. Supplementary calculations indicate that the first effect is small for the test cylinder. The calculations indicate that the stiffness $D_x$ is increased only about 3 percent by the rings; hence buckling pressure would be increased only $1\frac{1}{2}$ percent. The second effect is considered in reference 9, which indicates that the calculated buckling pressure is increased 10 percent by the resistance of the rings to rolling. The 10-percent increase may be somewhat high for the test cylinder because, here again, the calculation was made with the assumption that ring properties were smeared out, an assumption of questionable validity for the test cylinder.

6

Contemporary design procedures (derived in refs. 10 and 11 and used in refs. 12 to 14, for example) for the buckling strength of hydrostatically loaded ring-stiffened cylinders predict buckling pressures not much different from the calculated pressure of figure 7 for m = 1, the principal difference being that eccentricity of rings is incorporated into the calculation of figure 7 whereas it is not in references 10 and 11. Hence, figure 7 depicts a serious shortcoming of contemporary design procedures for ring-stiffened cylinders subjected to hydrostatic pressure. Such equations are derived on the assumption that the cylinder under hydrostatic pressure buckles in a mode with a single half wave in the axial direction (m = 1), an assumption carried over from experience on unstiffened cylinders. The addition of rings invalidates this assumption and its use is seen to lead to large unconservative errors in the predicted strength of cylinders. In this regard, it may be noted that the potential error is considerably greater than that depicted in figure 7. The buckling pressure in the m=1 mode is nearly inversely proportional to cylinder length; buckling pressure in the n=0 mode is independent of cylinder length unless extremely short cylinders are considered. Hence, calculations for cylinders progressively shorter than the test cylinder would indicate progressively greater differences between the calculated pressures for the two modes.

## CONCLUDING REMARKS

The results of a buckling test of a ring-stiffened cylinder loaded "hydrostatically" by external air pressure are presented and discussed. The cylinder failed catastrophically at a pressure corresponding to approximately 76 percent of the pressure predicted on the basis of classical small-deflection buckling theory that takes into account the one-sidedness of the reinforcing rings but averages their effects over the ring spacing. The cause of the 24-percent discrepancy between calculation and test was not determined from the investigation but is probably associated with initial imperfections, prebuckling deformations, and incompatibility of the buckle mode with the assumption of "smeared" rings, all of which were shown to exist in the test cylinder. The calculated pressure was considerably less than that predicted with the use of contemporary design equations for ring-stiffened cylinders and hence reveals a serious shortcoming of the equations.

Langley Research Center,
    National Aeronautics and Space Administration,
        Langley Station, Hampton, Va., June 27, 1966.

# APPENDIX

## CONVERSION OF U.S. CUSTOMARY UNITS TO SI UNITS

The International System of Units (SI) was adopted by the Eleventh General Conference on Weights and Measures, Paris, October 1960, in Resolution 12 (ref. 3). Conversion factors for the units used in this report are given in the following table:

| Physical quantity | U.S. Customary Unit | Conversion factor (*) | SI Unit |
|---|---|---|---|
| Length . . . . . . . | in. | 0.0254 | meters (m) |
|  | ft | 0.3048 | meters (m) |
| Modulus . . . . . . | ksi | $6.895 \times 10^6$ | newtons/meter$^2$ (N/m$^2$) |
| Pressure . . . . . | psi | $6.895 \times 10^3$ | newtons/meter$^2$ (N/m$^2$) |

*Multiply value given in U.S. Customary Units by conversion factor to obtain equivalent value in SI Units.

Prefixes to indicate multiple of units are as follows:

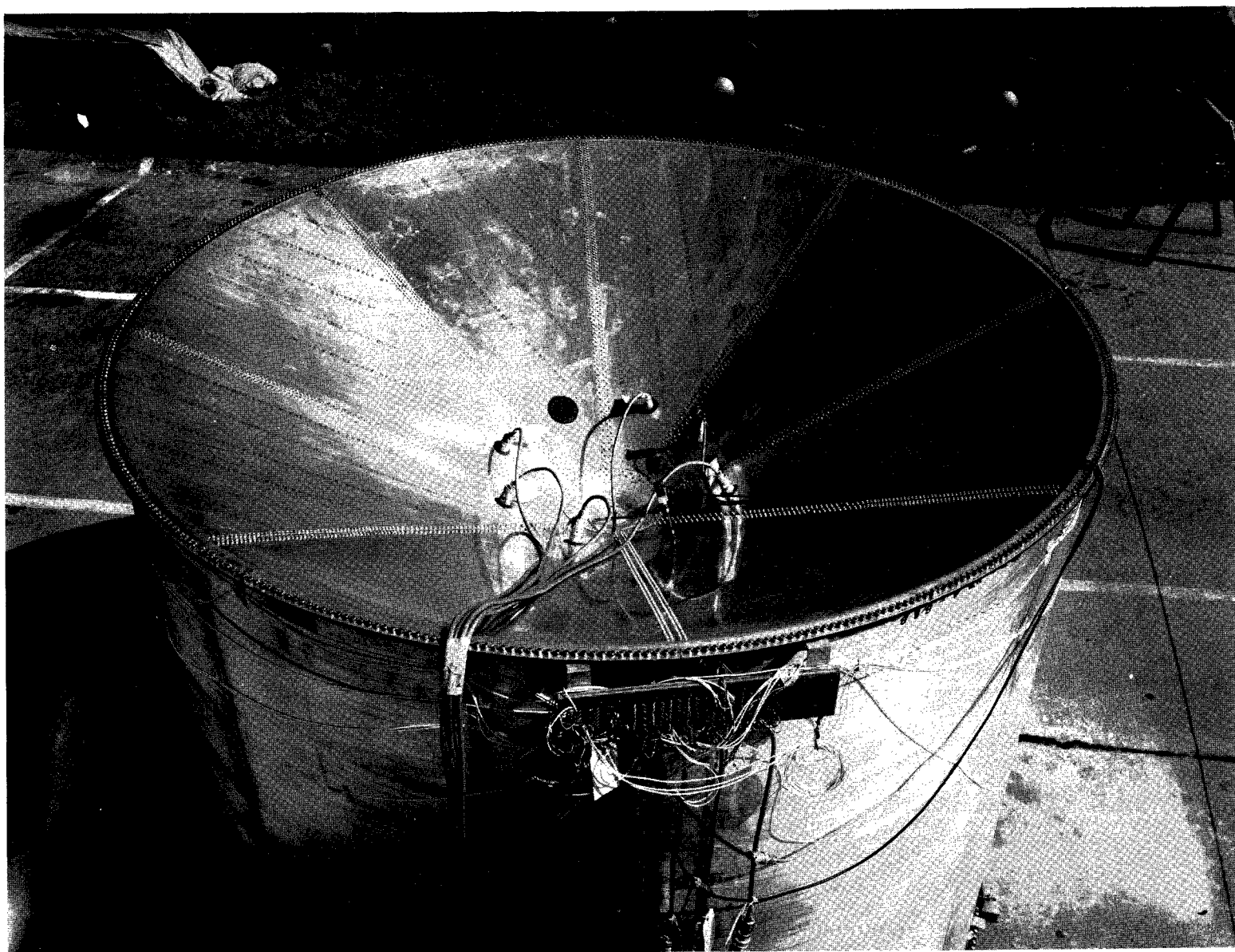| Prefix | Multiple |
|---|---|
| giga (G) | $10^9$ |
| kilo (k) | $10^3$ |
| centi (c) | $10^{-2}$ |
| milli (m) | $10^{-3}$ |

# REFERENCES

1. Windenburg, Dwight F.; and Trilling, Charles: Collapse by Instability of Thin Cylindrical Shells Under External Pressure. Trans. ASME, vol. 56, no. 11, Nov. 1934, pp. 819-825.

2. Dow, Donaldson A.: Buckling and Postbuckling Tests of Ring-Stiffened Circular Cylinders Loaded by Uniform External Pressure. NASA TN D-3111, 1965.

3. Mechtly, E. A.: The International System of Units — Physical Constants and Conversion Factors. NASA SP-7012, 1964.

4. Peterson, James P.; and Dow, Marvin B.: Structural Behavior of Pressurized, Ring-Stiffened, Thin-Wall Cylinders Subjected to Axial Compression. NASA TN D-506, 1960.

5. Block, David L.; Card, Michael F.; and Mikulas, Martin M., Jr.: Buckling of Eccentrically Stiffened Orthotropic Cylinders. NASA TN D-2960, 1965.

6. Stein, Manuel: The Influence of Prebuckling Deformations and Stresses on the Buckling of Perfect Cylinders. NASA TR R-190, 1964.

7. Fischer, G.: Über den Einfluss der gelenkigen Lagerung auf die Stabilität dünnwandiger Kreiszylinderschalen unter Axiallast und Innendruck. Z. Flugwissenschaften, Jahrg. 11, Heft 3, Mar. 1963, pp. 111-119.

8. Almroth, B. O.: Influence of Edge Conditions on the Stability of Axially Compressed Cylindrical Shells. NASA CR-161, 1965.

9. McElman, John A.: Eccentrically Stiffened Shallow Shells. PhD Thesis, Virginia Polytech. Inst., 1966.

10. Bodner, S. R.: General Instability of a Ring-Stiffened, Circular Cylindrical Shell Under Hydrostatic Pressure. J. Appl. Mech., vol. 24, no. 2, June 1957, pp. 269-277.

11. Becker, Herbert: General Instability of Stiffened Cylinders. NACA TN 4237, 1958.

12. Becker, Herbert: Handbook of Structural Stability. Part VI — Strength of Stiffened Curved Plates and Shells. NACA TN 3786, 1958.

13. Gerard, George: Minimum Weight Design of Ring Stiffened Cylinders Under External Pressure. J. Ship Res., vol. 5, no. 2, Sept. 1961, pp. 44-49.

14. Nickell, E. H.; and Crawford, R. F.: Optimum Ring Stiffened Cylinders Subjected to a Uniform Hydrostatic Pressure. [Preprint] 578F, Soc. Automotive Engrs., Oct. 1962.
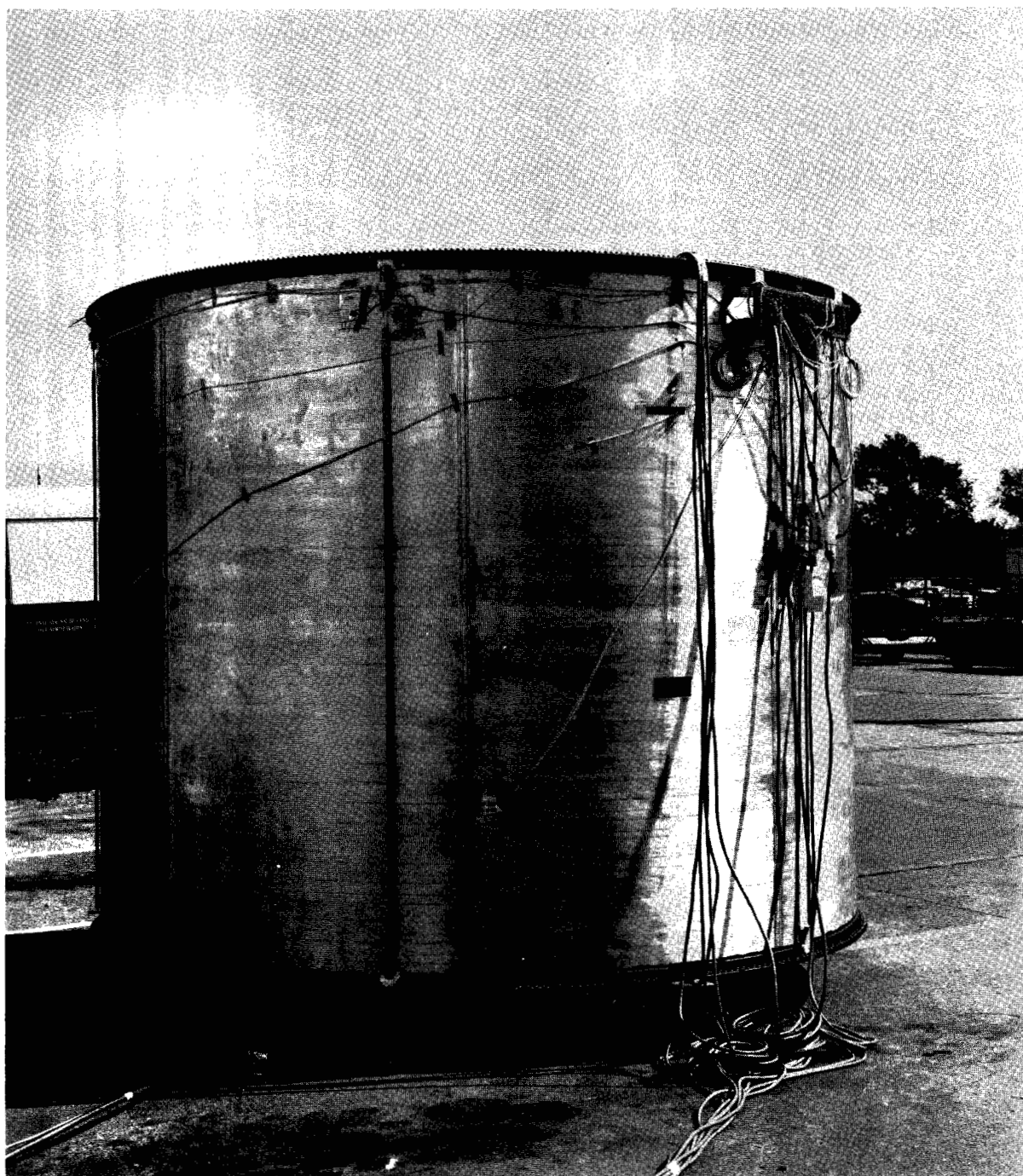
(a) General view.

L-65-7455

Figure 1.- Ten-foot-diameter (3-meter) test cylinder.

(b) View of end closure.

L-65-7454

Figure 1.- Continued.

(c) View of stiffening rings.
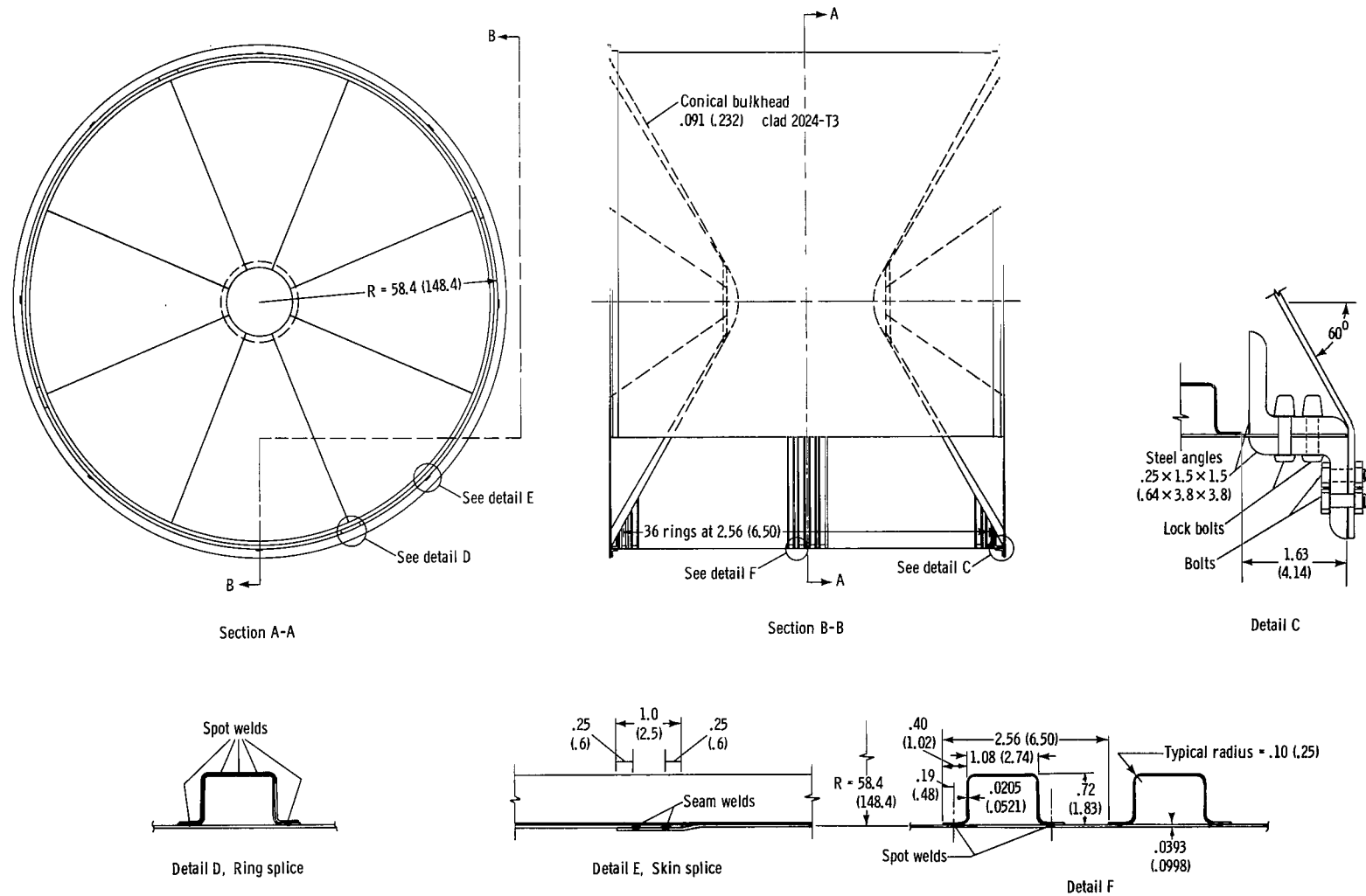
L-65-4321

Figure 1.- Concluded.

**Section A-A**

Conical bulkhead
.091 (.232)   clad 2024-T3

R = 58.4 (148.4)

See detail E

See detail D

36 rings at 2.56 (6.50)

See detail F

See detail C

**Section B-B**

60°

Steel angles
.25 × 1.5 × 1.5
(.64 × 3.8 × 3.8)

Lock bolts

Bolts

1.63
(4.14)

**Detail C**

Spot welds

**Detail D, Ring splice**

.25
(.6)

1.0
(2.5)

.25
(.6)

Seam welds

R = 58.4
(148.4)

**Detail E, Skin splice**

.40
(1.02)

2.56 (6.50)

1.08 (2.74)

.19
(.48)

.0205
(.0521)

.72
(1.83)

Typical radius = .10 (.25)

Spot welds

.0393
(.0998)

**Detail F**

Figure 2.- Construction details of test cylinder. Dimensions are in inches (centimeters).
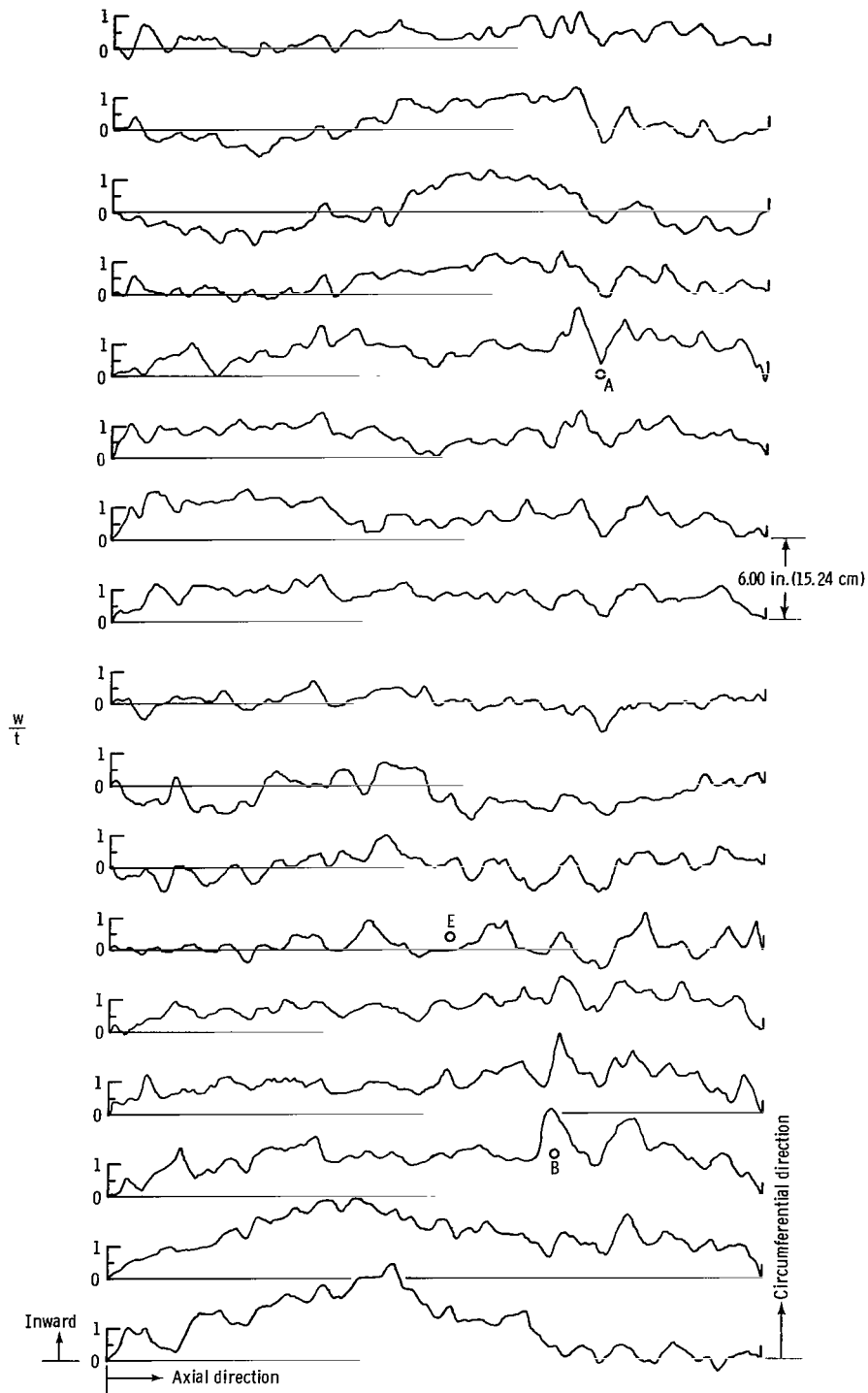
Figure 3.- Scanner plots showing initial imperfections of test cylinder. The 17 plots shown cover approximately 1/4 of the circumference of the cylinder. A, B, and E denote strain-gage locations.
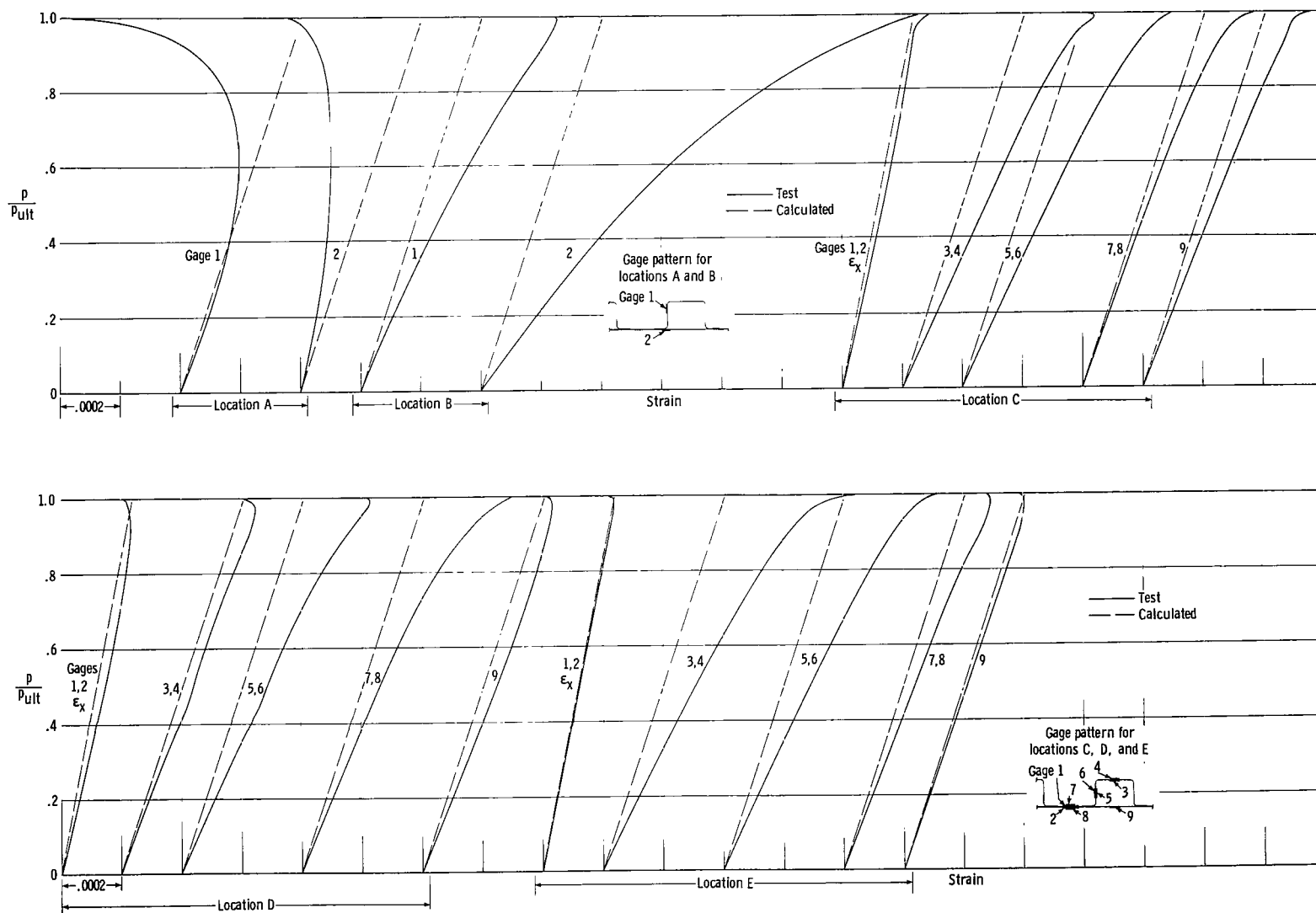
Figure 4.- Typical strain-gage data from test. All strains are circumferential strains except as noted.
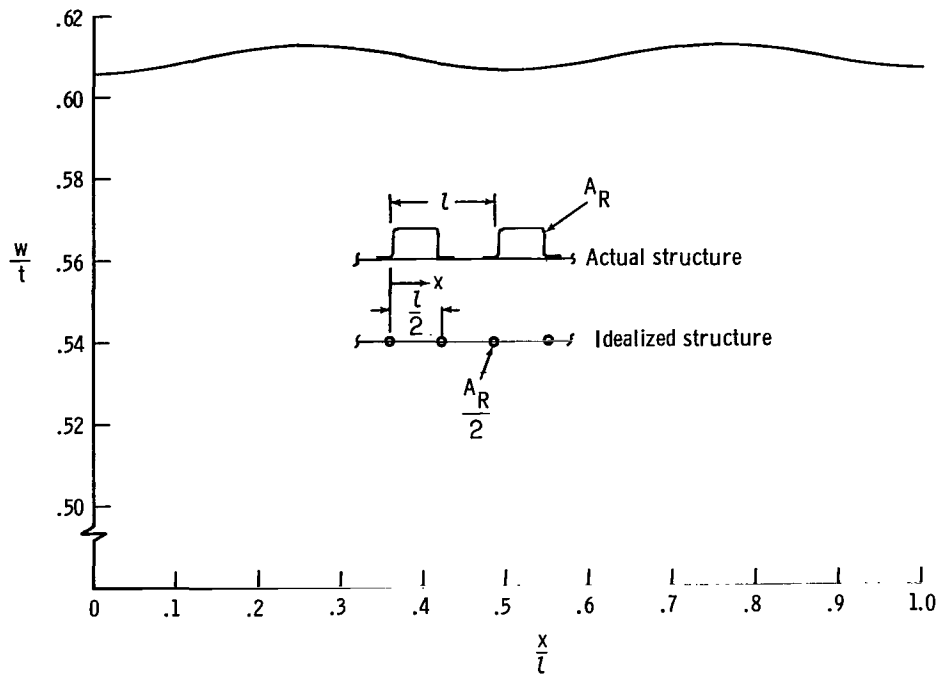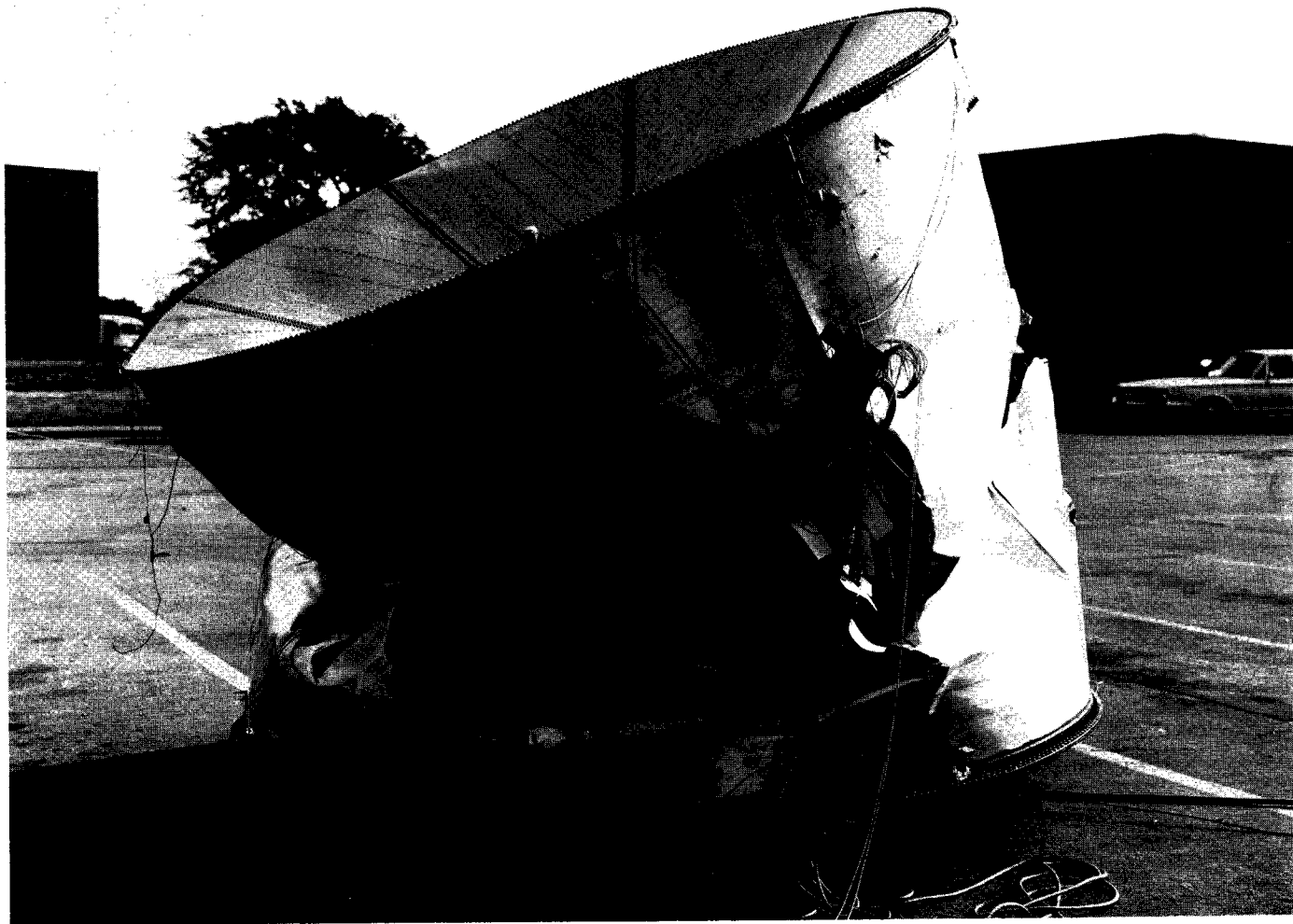
(a) Deformation of a typical wall section away from end ring.
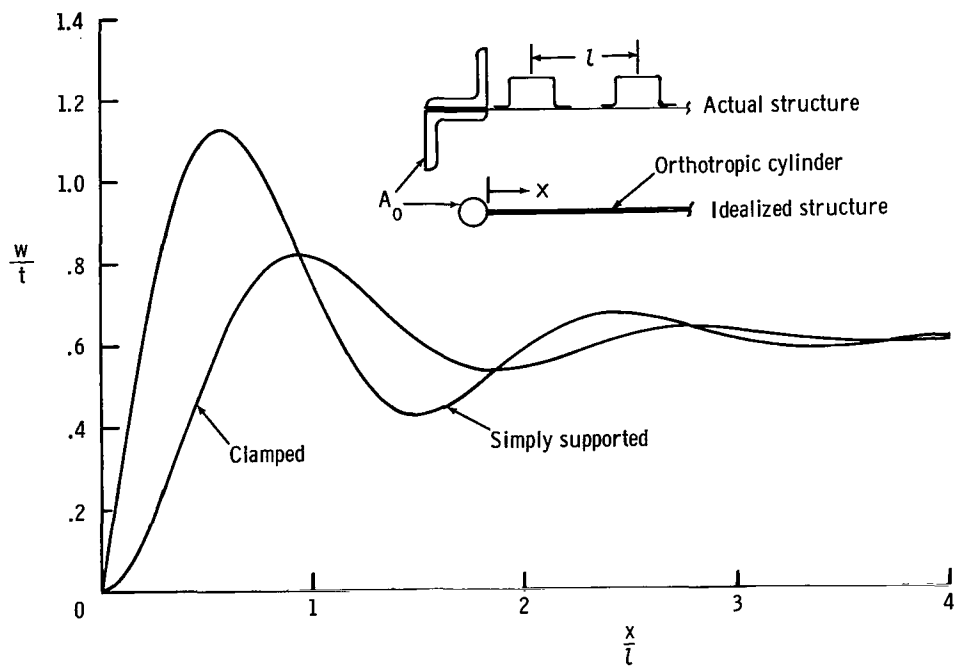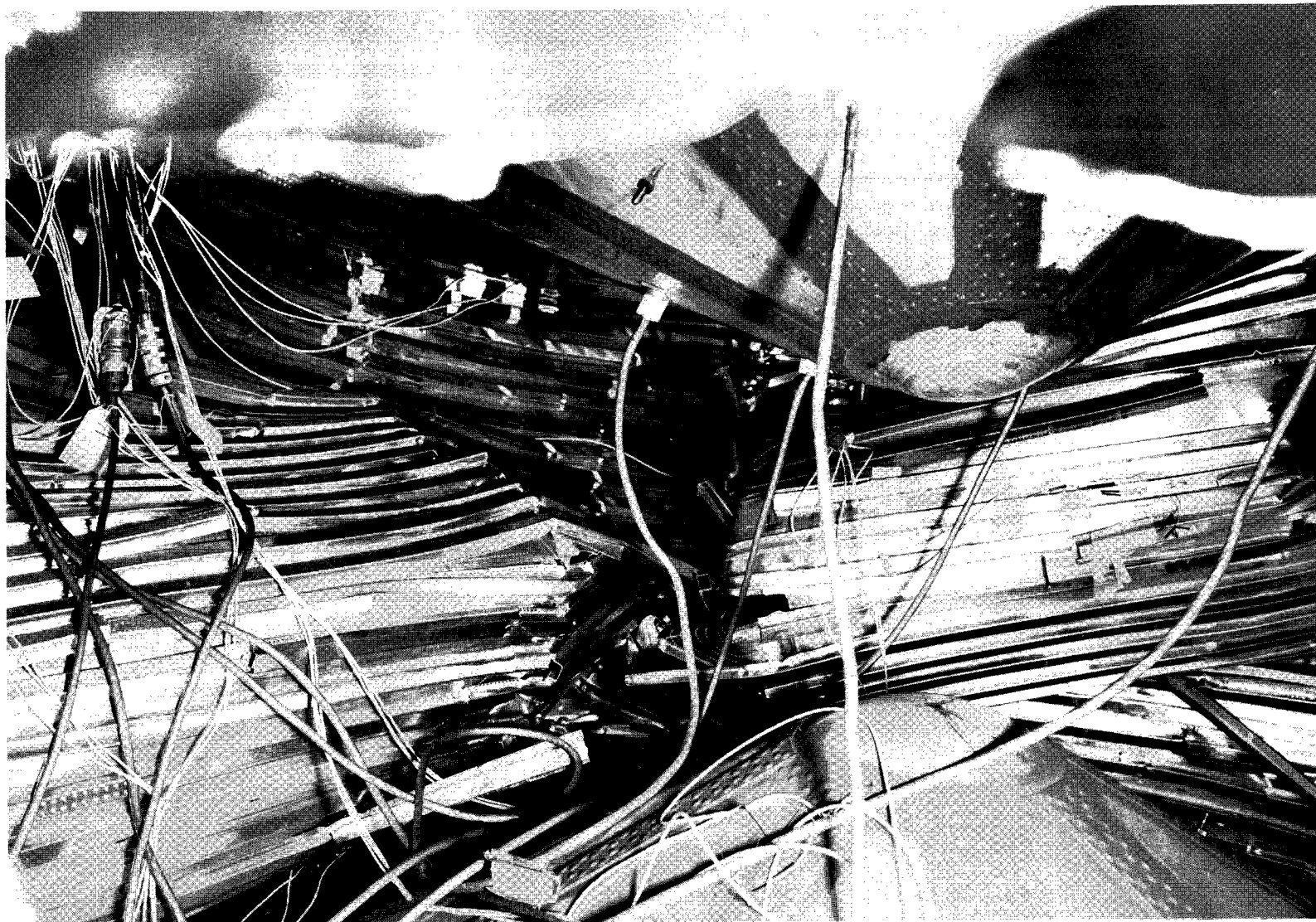


(b) Deformation near end ring.

Figure 5.- Calculated prebuckling deformations of test cylinder.

(a) General view.

Figure 6.- Test cylinder after failure.

L-65-7625

17

(b) View of inside cylinder.
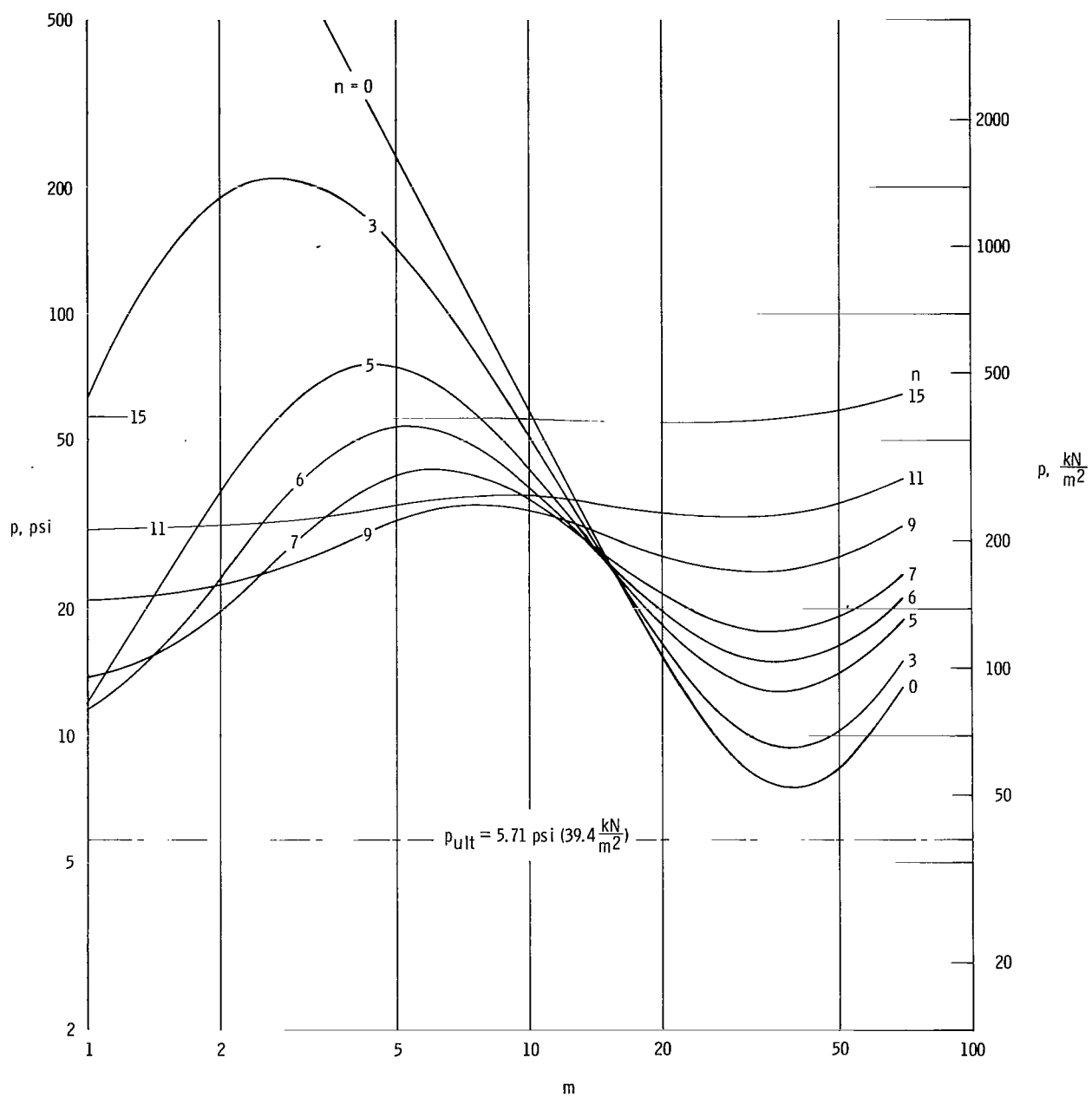
L-65-7628

Figure 6.- Concluded.

Figure 7.- Calculated buckling modes of test cylinder.

# NASA SCIENTIFIC AND TECHNICAL PUBLICATIONS

TECHNICAL REPORTS: Scientific and technical information considered important, complete, and a lasting contribution to existing knowledge.

TECHNICAL NOTES: Information less broad in scope but nevertheless of importance as a contribution to existing knowledge.

TECHNICAL MEMORANDUMS: Information receiving limited distribution because of preliminary data, security classification, or other reasons.

CONTRACTOR REPORTS: Technical information generated in connection with a NASA contract or grant and released under NASA auspices.

TECHNICAL TRANSLATIONS: Information published in a foreign language considered to merit NASA distribution in English.

TECHNICAL REPRINTS: Information derived from NASA activities and initially published in the form of journal articles.

SPECIAL PUBLICATIONS: Information derived from or of value to NASA activities but not necessarily reporting the results of individual NASA-programmed scientific efforts. Publications include conference proceedings, monographs, data compilations, handbooks, sourcebooks, and special bibliographies.

*Details on the availability of these publications may be obtained from:*

SCIENTIFIC AND TECHNICAL INFORMATION DIVISION

# NATIONAL AERONAUTICS AND SPACE ADMINISTRATION

Washington, D.C. 20546